THE JOURNAL OF PHYSICAL CHEMISTRY A

Article

pubs.acs.org/JPCA

Spectroscopy and Dynamics of Jet-Cooled Polyynes in a Slit Supersonic Discharge: Sub-Doppler Infrared Studies of Diacetylene HCCCCH

Chih-Hsuan Chang and David J. Nesbitt*

JILA, National Institute of Standards and Technology University of Colorado, and Department of Chemistry and Biochemistry, University of Colorado at Boulder, Boulder, Colorado 80309, United States

ABSTRACT: Fundamental, bending (ν_6, ν_7, ν_8, ν_9), and CC-stretch (ν_2, ν_3) hot band spectra in the antisymmetric CH stretch (ν_4) region near 3330 cm^{-1} have been observed and analyzed for jet cooled diacetylene (HC≡C−C≡CH) under sub-Doppler conditions. Diacetylene is generated in situ in the throat of a pulsed supersonic slit expansion by discharge dissociation of acetylene to form ethynyl (C≡CH) + H, followed by radical attack (HC≡CH + C≡C−H) to form HC≡C−C≡CH + H. The combination of (i) sub-Doppler line widths and (ii) absence of spectral congestion permits rotational structure and Coriolis interactions in the ν_4 CH stretch fundamental to be observed and analyzed with improved precision. Of particular dynamical interest, the spectra reveal diacteylene formation in highly excited internal vibrational states. Specifically, multiple Π ← Π and Δ ← Δ hot bands built on the ν_4 CH stretch fundamental are observed, due to doubly degenerate bending vibrations [cis C≡C−H bend (ν_6), trans C−C≡C bend (ν_7), trans C≡C−H bend (ν_8) and cis C−C≡C bend (ν_9)], as well as a heretofore unobserved Σ ← Σ band assigned to excitation of ν_2 or $2\nu_3$ CC stretch. Boltzmann analysis yields populations consistent with universally cold rotations (T_{rot} ≈ 15 ± 5 K) and yet superthermal vibrations (T_{vib} ≈ 85−430 K), the latter of which is quite anomalous for the high collision densities in a slit jet expansion. In order to elucidate the physical mechanism for this excess vibrational excitation, high level ab initio CCSD(T) calculations have been pursued with explicitly correlated basis sets (V*n*Z-f12; n = 2,3) and extrapolated to the complete basis set (CBS) limit using MOLPRO quantum chemistry software. The results suggest that the extensive hot band structure observed arises from (i) highly exothermic CCH + HCCH addition to yield a strongly bent HCCHCCH radical intermediate (ΔH = −62.6 kcal/mol), followed by (ii) rapid fragmentation over a submerged transition state barrier (ΔH = −18.9 kcal/mol) to form vibrationally hot diacetylene + H products (ΔH = −25.6 kcal/mol), and consistent with crossed molecular beam studies by Kaiser et al. [Phys. Chem. Chem. Phys. **2002**, *4*, 2950.] Finally, RRKM fragmentation rates for this complex are calculated, which exceed collision frequencies in the slit jet expansion and suggest near unity quantum efficiency for diacetylene formation.

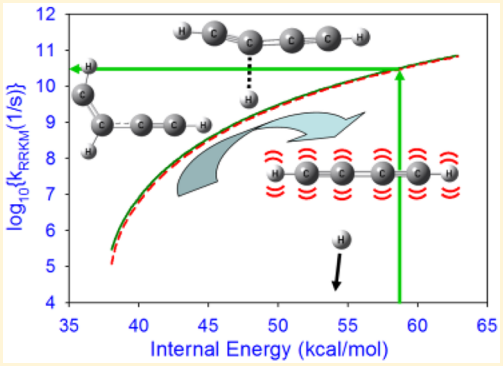

I. INTRODUCTION

Diacetylene (H−C≡C−C≡CH) is the smallest member of the polyyne family and represents an ubiquitous species in the combustion chemistry of unsaturated hydrocarbons and fuel rich flames.[1−4] What makes these linear polyynes so chemically interesting is the fact that they form readily via addition with CCH ethynyl radical, e.g.,

$$\begin{aligned} &HC{\equiv}CH' + C{\equiv}C{-}H \\ &\quad \rightarrow [H{-}C{\equiv}C(H'){-}C{\equiv}C{-}H] \\ &\quad \rightarrow H{-}C{\equiv}C{-}C{\equiv}C{-}H + H' \end{aligned} \tag{1a}$$

where the subsequent regeneration of CCH to complete the chain reaction can occur via additional H atom abstraction, for example,

$$H + H{-}C{\equiv}C{-}H \rightarrow H_2 + C{\equiv}C{-}H \tag{1b}$$

at sufficiently elevated temperatures.[5] It is worth noting here that the intermediate H−C≡C(H)−C≡C−H species is not a high energy transition state, but rather a stable radical adduct, ≈ 63 kcal/mol lower in energy than HCCH + CCH reactants, with little or no barrier to insertion and therefore resulting in a reaction rate constant at the near gas kinetic limit.[1,5−9] This process can continue by subsequent exothermic attack of CCH into one of the diacetylenic C≡C bonds, which then can form even higher order polyynes such as triacetylene, tetraacetylene, etc.[10] Indeed, such chain reaction kinetics are extremely rapid

Special Issue: 100 Years of Combustion Kinetics at Argonne: A Festschrift for Lawrence B. Harding, Joe V. Michael, and Albert F. Wagner

Received: March 9, 2015
Revised: April 23, 2015
Published: April 28, 2015

DOI: 10.1021/acs.jpca.5b02310
J. Phys. Chem. A 2015, 119, 7940−7950

under nonoxidizing flame conditions at normal pressures and temperatures, which therefore makes diacetylene (as well as each of the successive polyynes) a key crucial intermediate in the formation chemistry of soot.[10−14]

In yet another arena, diacetylene is a molecule of significant astrophysical interest.[7,15−19] In particular, the strong electronic absorption bands of diacetylene in the near UV play an important role in atmospheric chemistry of the outer planets and their respective moons, specifically shielding the planet surface from intense solar radiation, much like what the ozone layer achieves to control photochemistry in the earth's atmosphere. A classic example of this can be seen in the largest of Saturn's moons, Titan, whose atmosphere is thought to be dominated by acetylene chemistry and for which the surface looks orange due to "haze" forming photochemical reactions.[20,21]

By symmetry, diacetylene has a vanishing dipole moment, which makes it spectroscopically invisible to microwave/radio astronomical detection.[22,23] As a result, astrophysical search for such cumulated polyynic molecules in both nearby planetary as well as distant interstellar environments relies on vibrational spectroscopy in the midand near-infrared part of the spectrum. In particular, the strongly IR active antisymmetric CH stretch mode in such polyynes was the means for initial spectroscopic identification of acetylene in the atmosphere of Titan.[24,25] Interestingly, however, despite the clear acetylene content inferred from earth-based IR telescopes, evidence even for the simplest diacetylene adduct species was not available until the Voyager fly by mission.[26] Even more detailed spectroscopic data was made possible by the recent Cassini spacecraft,[25] which provided direct identification of diacetylene based on the characteristic absorption bands of the antisymmetric C−H stretch(ν_4), cis H−C≡C bend(ν_6), and trans H−C≡C bend(ν_8) in the spectra at 3333, 625, and 627 cm^{-1} Furthermore, since exposure of these polyynes to solar VUV radiation yields highly reactive radical CCH fragments, this provides a photolysis mechanism for radical chain production of higher and higher molecular weight species, which indeed are proposed as key intermediates in the formation of organic aerosols (tholines),[27] soot formation,[11] and polycyclic aromatic hydrocarbons (PAH).[28]

As a result of such interest, the vibrational spectroscopy of diacetylene has been the subject of intense infrared and Raman investigations (see Table 1).[29−33] The pioneering infrared study by Guelachvili et al.[29] has reported Fourier transform absorption spectra of diacetylene in the 1850−2523 and 2860−3584 cm^{-1} windows, corresponding to $\Delta\nu = 1$ transitions in the antisymmetric C≡C (ν_5) and CH (ν_4) stretch regions, respectively. In their work, full spectral analysis and rovibrational constants were obtained for (i) the ν_4 and ν_5 fundamentals, (ii) a plethora of hot bands arising from C≡C(ν_5) and CH(ν_4) stretch excitations built on the thermally populated ν_6 cis CCH bend, the ν_7 trans CCC bend, the ν_8 trans CCC bend, and the ν_9 cis CCH bend lower states, (iii) as well as multiple stretch + bend combination bands. For the ν_4 antisymmetric CH stretch mode of specific interest to the present work, the bending hot bands could be assigned to combinations of 6^1_1, 7^1_1, 9^1_1 and $9^2_2(\Sigma)$ with 4^1_0, where we have borrowed from conventional vibronic notation to indicate the number of lower/upper quanta and symmetry label in each vibrational mode. Interestingly, no hot bands associated with the trans CCH bend mode (e.g., $4^1_0 8^1_1$) were reported, presumably due to spectral congestion under room temperature and Doppler limited conditions. Nevertheless, the corresponding Π−Π hot bands for all four bending states (ν_6, ν_7, ν_8, and ν_9) built on the ν_5 CCC asymmetric stretch band were observed, as well as a progression of multiquanta hot band excitations with the ν_9 cis CCC bending mode.

Combination bands observed include the excitation of a series of bending modes, such as ν_1, ν_6, and ν_8, as well as ν_5, ν_6, and ν_9. The $\nu_6+\nu_8$ combination band at 1250 cm^{-1} was studied by Matsumura et al.[34] by Stark modulation infrared diode spectroscopy, with the same band measured by McNaughton and Bruget.[35] Also observed were other combination bands building on the $\nu_6 + \nu_8$ level. Arié and Johns[30] reported the two bending energy levels of $(\nu_8, \nu_9)^k$ mode, where $k \equiv l_8 + l_9$, and l_8 and l_9 are the corresponding vibration angular momenta. Recently, Bizzocchi et al.[31] investigated spectral bands of diacetylene and diacetylene-d_2 extended into submillimeter-wave $\nu_8-\nu_6$ region, and its ν_9-associated hot band. Interactions between the $\nu_3 = 1$ stretching mode, the $\nu_8 = \nu_9 = 1$ combination, and $\nu_7 = 2$ level have been analyzed by the same group[32] in terms of vibrational l-type resonances and cubic anharmonic coupling. The full set of normal mode vibrations and associated frequencies for diacetylene are summarized in Table 1.

Difference band microwave spectra for vibration−rotational transitions between closely spaced bending states have also been reported by Matsumura and Tanaka.[36] In particular, the $\nu_8-\nu_6$ and $\nu_8+\nu_9-\nu_6-\nu_9$ difference bands have been successfully analyzed, which require inclusion of l-type and Fermi resonance interactions, with the transition dipole moment for these $\Sigma_g^+-\Sigma_u^+$ and $\Sigma_g^--\Sigma_u^-$ sub-bands of the $\nu_8+\nu_9-\nu_6-\nu_9$ difference frequency vibration determined to be ≈ 0.075 D by Stark effect studies.[34,37] Furthermore, Matsumura and Tanaka[38,39] indicated higher order dipole moment derivatives with respect to the cis/trans C≡C−H bending coordinates to be quite significant, which generates additional non-negligible transition moments for overtone, combination, and difference bands involving the ν_6 and ν_8 mode. Recently, the Linnartz group has made a systematic investigation of diacetylene in the CH stretch region using high-resolution cavity ring down methods in a planar discharge expansion source.[33] Of particular interest is their observation of nonequilibrium excitation of diacetylene in multiple degenerate CCC and CH bending modes even under relatively cold, planar expansion conditions. This proves especially relevant to the present study, which provides additional spectroscopic characterization of the diacetylene product with sub-Doppler instrumental resolution (60 MHz)

Table 1. Frequencies/Symmetries for the Fundamental Modes of Diacetylene

mode	symmetry	vibrational motion	frequencies
ν_1	Σ_g^+	Sym C−H stretch	3332.1541[a]
ν_2		Sym C≡C stretch	2188.9285
ν_3		C−C stretch	871.9582[a]
ν_4	Σ_u^+	Asym C−H stretch	3333.6647[b]
ν_5		Asym C≡C stretch	2022.2415[b]
ν_6	Π_g	H−C≡C bend	625.6436
ν_7		C≡C−C bend	482.7078[a]
ν_8	Π_u	H−C≡C bend	627.89423(10)[a]
ν_9		C≡C−C bend	219.97713(10)[a]

[a]E. Arie and J. W. C. Johns, J. Mol. Spec. **1992**, *155*, 195. [b]Guelachvili et al. J. Mol. Spec. **1984**, *105*, 156.

DOI: 10.1021/acs.jpca.5b02310
J. Phys. Chem. A 2015, 119, 7940−7950

and improved frequency precision (7 MHz) as well as high-level ab initio quantum mechanical support for a Franck−Condon-like origin of such nonequilibrium vibrational dynamics in the formation event, and in good agreement with the high internal energy distributions ($\langle E_{int} \rangle \approx 14 \pm 3$ kcal/mol) noted in crossed molecular beam studies of Kaiser et al.[7]

Specifically, in this work, diacetylene (HC≡C−C≡CH) is formed and investigated via sub-Doppler infrared difference frequency spectroscopy under supersonically cooled, discharge slit jet expansion conditions. Diacetylene is generated in situ in the throat of a pulsed supersonic slit expansion by discharge dissociation of acetylene to form ethynyl (C≡CH) + H, followed by radical attack (HC≡CH + C≡C−H) to form HC≡C−C≡CH + H. Spectroscopically, the sub-Doppler resolution data provide clear evidence for a "local" Π−Σ Coriolis perturbation due to a rotationally avoided crossing in the antisymmetric CH stretch fundamental (ν_4), which provides an improved analysis of the diacetylene spectra for low J states preferentially populated in the slit jet. We also take the opportunity to analyze low frequency doubly degenerate bending states (ν_6,ν_7,ν_8,ν_9) at sub-Doppler resolution and compare with results from extensive previous spectroscopic studies by Guelachvili et al.[29] and Zhao et al.[33] Furthermore, we observe additional Σ−Σ bands in the slit jet, which we ascribe to ν_4 hot band spectra built on CC-stretch (ν_2 or $2\nu_3$) excitation in the lower state. Of special interest is investigating the dynamical reason for the presence of such vibrationally hot spectra observed under slit jet expansion conditions, specifically the significant population of the Π degenerate bends [cis C≡C−H bend (ν_6), trans C−C≡C bend (ν_7), trans C≡C−H bend (ν_8) and cis C−C≡C bend (ν_9)], as well as hot band excitation out of Σ symmetry CC stretch vibrational manifold. As an important secondary focus of this work, therefore, we explore and provide theoretical support for such non-equilibrium vibrational dynamics by high level ab initio CCSD(T)/VnZ-f12 calculations of the complex transition state geometry, energetics, and vibrational frequencies for predictions of RRKM lifetimes.[6,40−43]

II. EXPERIMENTAL SECTION

The sub-Doppler slit jet discharge infrared spectrometer has been thoroughly described elsewhere[44−46] and only requires brief summary of details relevant to the current study. High-resolution IR light (<2 MHz, 3−5 μW) is formed by difference-frequency generation (DFG) of a tunable single mode ring-dye laser (Spectra-Physics 380A, R6G dye) with a fixed-frequency single mode Ar^+ laser (Spectra-Physics Series 2000, 488 nm) within a temperature-controlled, periodically poled $LiNbO_3$ (PPLN) crystal. This IR light is split into a reference and signal beam for fast analog subtraction of common mode amplitude noise, with the signal beam directed through the slit discharge expansion region to monitor jet cooled diacetylene and focused onto a liquid N_2 cooled InSb detector. The transient absorptions are measured in a 16-fold Herriot cell multipass 5 mm downstream of the long axis of the slit jet expansion, with the diacetylene concentrations modulated with a 500 V/200 mA discharge operating at 50 kHz. The multipass is aligned to achieve a tight bundle of beams (5 mm diameter), in order to minimize averaging over different spatial domains of the expansion. Of special importance, collisions in the slit jet expansion quench Doppler broadening along the slit axis down to 60 MHz, which results in naturally sub-Doppler spectroscopy without the need for nonlinear saturation techniques. Frequency measurements reflect results of multiple scans over the same region and are obtained via fringe interpolation on a laser stabilized optical marker cavity. Absolute frequencies are obtained with respect to ν_3 $R(2)$, $R(3)$ and $R(4)$ transitions acetylene[47] at 3301.848040, 3304.166740, and 3306.476227 cm^{-1}, respectively. The uncertainty of the spectral measurements is experimentally determined to be 7 MHz (0.00023 cm^{-1}), obtained from the standard deviation of repeated absolute frequency measurements over several weeks of data collection/analysis.

The jet-cooled diacetylene molecules are generated by discharge of a mixture of 0.1% of acetylene in a 70%:30% Ne−He (Ne-70) buffer gas through a pulsed-slit (300 μm × 4 cm), with a 19 Hz repetition rate and 1 ms pulse duration. From a sudden approximation perspective, the desired adduct species is formed via barrierless attack[6,7,19] of the ethynyl (CCH) radical onto acetylene, followed by prompt ejection of the adjacent H atom to form highly bend and stretch excited diacetylene.[42,43] For typical quantum state resolved densities in the slit jet expansion, peak absorption strengths for diacetylene are 0.4%, which, at near shot noise limited sensitivities of 2×10^{-5}, yield typical signal-to-noise ratios in excess of 100:1.

III. RESULTS AND ANALYSIS

A. Spectroscopic Background. Diacetylene is formed in the slit jet discharge from rapid reactive collisions of ethynyl radical with acetylene to form HCCCCH + H. This newly formed diacetylene cools rotationally down in the Ne-70 expansion diluent to low rotational temperatures, which results in an intense progression of lines in the 3333 cm^{-1} region of the ν_4 fundamental. As shown in Table 1, only vibrations with Σ_g^+ and Π_u symmetry are infrared active. For the Σ−Σ transitions, only P and R branches have oscillator strength, which display the characteristic intensity alternation due to 3:1 *ortho* (J = even) and *para* (J = odd) nuclear spin statistical weights for equivalent H atoms. For Π−Π and Δ−Δ transitions, the rotational levels can exhibit additional structure due to excitation of a 2-fold degenerate bending mode. Coupling between vibrational (l) and rotational (N) angular momentum results in l-type doubling for each rotational level. Specifically, the rotational states for each $J = l + N$ are split into two components with e/f[48] energy separation characterized by $qJ(J+1)$, where q is the l-type doubling constant. We also see additional spectral progressions due to other unsaturated polyyne species in the jet. However, these are typically at much reduced concentrations and can be cleanly distinguished from diacetylene by rotational spacings.

B. Asymmetric CH Stretch (ν_4) Fundamental and Perturbations. We begin with spectroscopic analysis of the jet cooled sub-Doppler ν_4 asymmetric stretch spectrum. Although this band has been studied extensively with Fourier transform and supersonic jet methods, the present detection under sub-Doppler resolution conditions reveals the presence of perturbing level shifts not observed previously.[29,33] As shown in Figure 3 (upper panel), the spectra provide clear evidence for an "avoided crossing" due to coupling to a perturbing rotational progression, which yields systematic positive and negative shifts in the fitted residuals. The location of this perturbation is confirmed by observation of identical shifts via both P and R branch access to the same upper N, which unambiguously implies the interaction takes place in the vibrationally excited state.[22,49] Given the small residuals and highly rotationally

DOI: 10.1021/acs.jpca.5b02310
J. Phys. Chem. A 2015, 119, 7940−7950

Table 2. Least Squares Fitting Results[a] (cm^{-1}) for Σ−Π Coriolis Deperturbation Analysis of the Antisymmetric CH Stretch (ν_4) Mode of Diacetylene (See Text for Details)

	ground level[b]	ν_4 (Σ^+_u)	ν_{pert} (Π)	ν_4 (Σ^+_u) (previous)[c]
B	0.14641118	0.1461926(2)[b]	0.146255(18)	0.1461929(4)
D	1.56825×10^{-8}	$1.477(13) \times 10^{-8}$		$1.506(24) \times 10^{-8}$
ν_0		3333.66338(2)	3333.6518(33)	3333.6634(1)
β_0			$6.9(9) \times 10^{-5}$	
σ		0.00014		

[a]Uncertainties in the parentheses are one standard deviation. [b]Ground state constants fixed at the precision FTIR values of Bizzocchi et al.[32] [c]Comparison results from Zhao et al.[33]

"local" nature of this crossing, the perturbation arises from Σ−Π ($K = 1 \leftrightarrow 0$) Coriolis coupling between the ν_4 upper state (Σ) with a dark Π_u vibrational manifold, the shifts from which can be analyzed with a simple 2 × 2 Coriolis Hamiltonian matrix.[22]

$$\begin{pmatrix} \nu_\Sigma + B_\Sigma J(J+1) - D_\Sigma J^2(J+1)^2 & \beta_0\sqrt{J(J+1)} \\ \beta_0\sqrt{J(J+1)} & \nu_\Pi + B_\Pi J(J+1) \end{pmatrix} \quad (2)$$

In eq 2, (i) $\nu_\Sigma + B_\Sigma J(J+1) - D_\Sigma J^2(J+1)^2$ describes the *unperturbed* rotational energy levels of ν_4 mode, (ii) ν_Π and B_Π are parameters representing the *perturbing* vibrational levels, with (iii) the J-dependent $(\beta_0(J(J+1))^{1/2})$ matrix element relevant for $K = 1 \leftrightarrow 0$ Coriolis interactions.[22] Finally, we also include in this least-squares analysis of the previous cavity ringdown[33] and Fourier transform spectral measurements[29] utilized in the earlier fits (see Supporting Information of Zhao et al.[33]), appropriately weighted by the inverse square of the reported measurement uncertainties. To be consistent with the previous analysis of Zhao et al.,[33] we furthermore fix the lower state B, D rotational constants at values well characterized by the low frequency Fourier transform studies of Bizzocchi et al.[32]

The deperturbation results for the ν_4 antisymmetric C−H stretch mode of diacetylene are summarized in Table 2. The band origin for the antisymmetric CH stretch is determined to be 3333.66338(2) cm^{-1}, in excellent agreement with the results of Linnartz and co-workers (3333.6634(1) cm^{-1}), despite evidence for small but systematic red shifts (-8×10^{-4} cm^{-1}) in the low J data from the early FTIR results.[29,33] Similarly, the band origin and rotational constant for the *perturbing* level is determined from the fit to be ν_Π = 3333.6518(33) cm^{-1} and B_Π = 0.146255(18) cm^{-1}, with a small Coriolis coupling coefficient, β_0 = 6.9(9) × 10^{-5} cm^{-1}. Noteworthy is the significantly positive fractional change in ΔB/B (+0.043%) with respect to the unperturbed excited state, which would be consistent with a vibrational bending of the linear CCCC backbone and therefore *decreased* projection of atomic masses along the A inertial axis. Although the large density of states in diacetylene at 3300 cm^{-1} precludes definitive assignment of the perturbing vibration, this density is dominated by the lowest frequency bending modes (ν_6, ν_7, ν_8, ν_9) that systematically *decrease* the effective moment of inertia for end over end rotation. Indeed, the observed *increase* in rotational constant for the perturbing vs deperturbed manifold is entirely consistent with these expectations.

C. Π−Π Hot Bands and Bending Vibrational Populations. What makes the slit discharge spectrum for diacetylene of particular dynamical interest, however, is the spectral evidence for extensive hot vibrational state populations in the spectra. Specifically, in addition to the strong progression noted above due to fundamental excitation of the antisymmetric C−H stretching mode (ν_4), the region between 3328−3340 cm^{-1} reveals a rich set of rotationally resolved spectra associated with ν_4 hot band excitation built on top of doubly degenerate bending vibrations populated in the expansion. Assignment of these hot bands to the four low frequency bending modes $4^1_0 6^1_1$, $4^1_0 7^1_1$, $4^1_0 8^1_1$, and $4^1_0 9^1_1$ is straightforward, both based on the previous work by Guelachvili et al.[29] as well as the recent study by Zhao et al.[33] A sample portion of the slit jet cooled diacetylene infrared absorption spectra near the fundamental ν_4 band origin is displayed in Figure 1, which

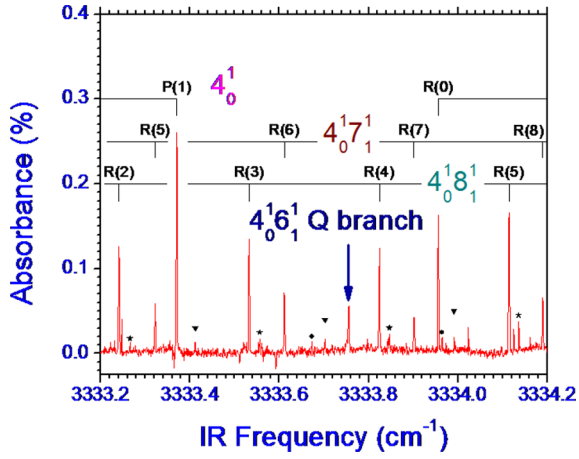

Figure 1. Sample sub-Doppler IR hot band spectra of diacetylene built on the ν_4 antisymmetric CH stretch fundamental, with rotational assignment indicated for the $4^1_0 7^1_1$ and $4^1_0 8^1_1$ hot band progressions. Symbols (★), (●), and (▼) highlight additional progressions due to the ν_9 bend ($4^1_0 9^1_1$), 2 quanta of ν_7 ($4^1_0 7^2_2(\Delta-\Delta)$), and a previously unobserved Σ−Σ hot band built on a collinear CC stretch vibration (assigned to $4^1_0 2^1_1$ or $4^1_0 3^2_2$ based on ΔB), respectively.

highlights a small portion of rotational progressions observed in $4^1_0 7^1_1$, $4^1_0 8^1_1$ bending hot bands. It is important to emphasize that these high steady state populations of excited bending states are formed and remain inefficiently cooled in a slit 1D expansion, which has a $1/r$ versus $1/r^2$ density drop off and therefore ≈ 2 orders of magnitude higher collisions than experienced in a traditional 2D pinhole nozzle expansion environment.[50−53]

Due to l-type doubling in each of the Π−Π bending hot bands, each of the sub-Doppler rotational progressions appears as unresolved transitions at low J values, which then split into two resolved components at sufficiently higher J = 10−15 (e.g., see Figure 2). The intensity ratios displayed for the two $R(11)$ line components arise from 3:1 nuclear spin weight alternation, which reverses ordering for J = even and odd lower states. The

DOI: 10.1021/acs.jpca.5b02310
J. Phys. Chem. A 2015, 119, 7940−7950

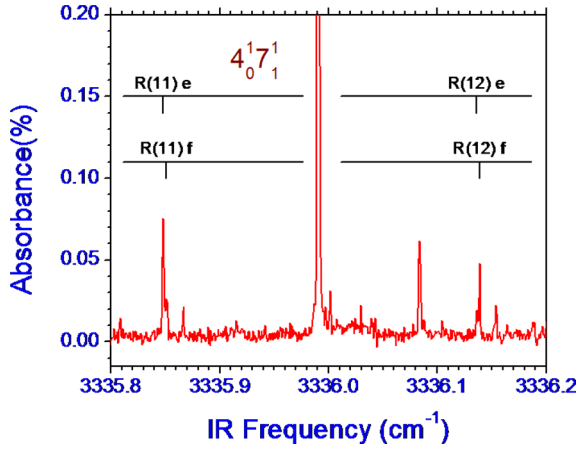

Figure 2. Sample blowup of $R(11)$, $R(12)$ $4_0^1 7_1^1$ rotational lines exhibiting l-type doubling due to e/f components in a Π symmetry vibrational state. Intensity alternation (3:1) in the resolved e/f components is due to (*ortho*/*para*) nuclear spin statistics for the identical H atoms. The strong peak near 3336 cm^{-1} is $R(5)$ of the 4_0^1 fundamental band.

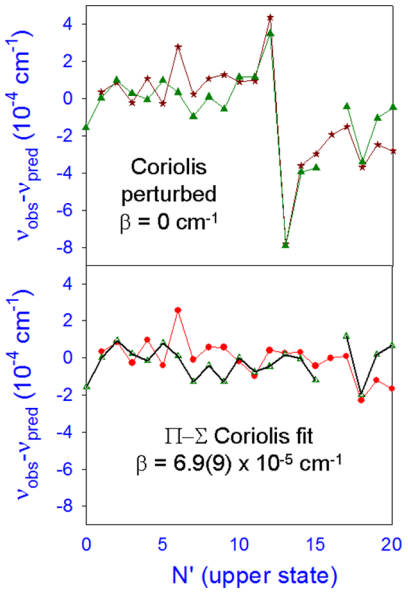

Figure 3. Upper panel: Least squares P/R branch fitting results for the antisymmetric CH stretching mode (ν_4) of jet cooled diacetylene, clearly revealing a "local" rotational crossing with a dark state of Π symmetry centered around $J' = 12$. Lower panel: P/R branch residuals from deperturbed fits that include Σ–Π Coriolis coupling explicitly in the Hamiltonian (see text for details).

rotational energies for the $\sum$ ($l = 0$) or Π ($l = 1$) manifold can be accurately characterized by a simple effective Hamiltonian

$$E(N) = \nu_0 + B[J(J+1) - l^2] - D[J(J+1) - l^2]^2 \pm q/2[J(J+1)] \quad (3)$$

where ν_0, B, and D represent band origin, rotational, centrifugal distortion constants, respectively, J is the total angular momentum, and q is the l-type doubling parameter.[22]

It is worth noting that the spectroscopic parameters for each of these four bending hot bands have been previously determined with the combination of low temperature/cavity ring down and high temperature/FTIR data of Zhao et al. and Guelachvili et al, respectively.[29,33] Indeed, our interest in these bands is mainly for the information on vibrational populations they provide. In the interest of completeness, however, we have performed weighted least-squares fits of the current sub-Doppler hot band transitions to eq 3, combined with the transitions reported by Zhao et al.[33] and Bizzocchi et al.,[32] with results summarized in Table 3. Rotational, centrifugal distortion and l-doubling constants for each of ν_6, ν_8, ν_9 lower bending states have been taken from recent FTIR studies of Dore and co-workers[32] and are held fixed. Inclusion of the current sub-Doppler transitions frequencies yields slightly more precise spectroscopic parameters (e.g., typically 2× improvement in vibrational band origins), but in essentially all cases within experimental error of the values reported previously.[33]

D. Σ–Σ and Δ–Δ Hot Bands. There are two additional bands observed to slightly lower frequencies, with weaker absorption intensities in comparison to those of the other hot bands mentioned above. Based on the close proximity to the other spectra, it is reasonable to presume that these two additional progressions are also associated with low frequency vibrational hot bands built on the antisymmetric CH stretch ν_4 mode. However, these bands reveal no resolved l-type doubling structure, which even for jet-cooled low J states is qualitatively different from the spectra noted in Section C and therefore eliminates Π–Π bending hot bands from consideration. The first band contains a weak Q branch feature and is missing P(1), P(2), R(0), and R(1) lines in the P/R branch rotational progression, i.e., characteristic of a Δ–Δ band type for which l-type doubling is present but too small to resolve under sub-Doppler jet cooled conditions. Indeed, comparison of the transition frequencies confirms this as a band previously observed by Linnartz and co-workers, which by ab initio analysis of the strong positive vibrational shift in B with respect to the vibrationless ground state ($\Delta B = +5.4 \times 10^{-4}$ cm^{-1}) was assigned to the $4_0^1 7_2^2$ Δ–Δ hot band.[33] The absence of lines in the present data with $J \leq 1$ provides further confirmation of the

Table 3. Fitting Results (cm^{-1}) for ν_4 Bend/Stretch Hot Bands of Jet Cooled Diacetylene[a]

band	ν_0	B'	$D' \times 10^8$	$q' \times 10^5$	B''	$D'' \times 10^8$	$q'' \times 10^5$	$\sigma^b \times 10^4$	ΔB^c x 10^4
$4_0^1 6_1^1$	3333.75595(5)[a]	0.1462555(2)	1.572(3)	−8.117(9)	0.14647893[d]	1.57471[d]	−8.289[d]	2.2	+0.668
$4_0^1 7_1^1$	3332.36315(4)	0.146462(1)	1.61(2)	−11.5(2)	0.146681(1)	1.61(2)	−11.5(2)	2.1	+2.698
$4_0^1 8_1^1$	3331.57275(11)	0.146260(3)	1.0(15)	−7.9(1)	0.14647473[d]	1.57479[d]	−8.03739[d]	2.9	+0.636
$4_0^1 9_1^1$	3333.08585(5)	0.1466151(5)	1.63(4)	−20.59(6)	0.146831(3)[d]	1.6288[d]	−20.532[d]	1.7	+4.186
$4_0^1 7_2^2$(Δ–Δ)	3331.07440(10)	0.146753(3)	3.3(4)	−0.0031(15)	0.146955(3)	1.568[e]	−0.0055(15)	2.5	+5.434
4_0^1 ? (Σ–Σ)[f]	3332.97420(5)	0.145602(2)	----	----	0.145822(2)	----	----	1.6	−5.895

[a]Includes all transitions with nonzero weights from Supporting Information from Zhao et al.[33] and Gualechvali et al.[29] Uncertainties in parentheses represent 1σ. [b]Standard deviation of the fit. [c]Change in lower state B with respect to vibrationless level. [d]Fixed at ground state values of Bizzocchi et al.[32] [e]Fixed at values determined by Bizzocchi et al.[32] [f]Tentative hot band assignment to ν_2 or $2\nu_3$ based on ΔB values and ab initio predictions.[55]

DOI: 10.1021/acs.jpca.5b02310
J. Phys. Chem. A 2015, 119, 7940–7950

Linnartz assignment, with a combined weighted least-squares fit to both sets of data yielding results summarized in Table 3. The *l*-doubling information in such spectra arise from the 3:1 predominance for *e*/*f* transitions out of even/odd *J* lower rotational states due to nuclear spin statistics. Thus, the observed Δ−Δ frequencies are fit to a linear molecule Hamiltonian with *J* even/odd energy levels shifted with a $\pm q/2(J+2)(J+1)J(J-1)$ dependence of the *l*-doubling appropriate for a lower state with $l = 2$.[52,54]

By way of contrast, the second band clearly exhibits 3:1 nuclear spin intensity alternation, shows no Q-branch feature and has a sub-Doppler progression which includes both P(1) and R(0) lines, i.e., unambiguously characteristic of a Σ−Σ band. This hot band does not match any bands reported previously, despite the absence under our slit jet discharge conditions of several other ν_4 hot bands seen by Zhao et al.[33] Consistent with a Σ−Σ band, least-squares fits of the transition frequencies to a linear molecule Hamiltonian have been performed, with the resulting band origin and rotational constants listed in Table 3. The lower state rotational constant for this Σ−Σ type transition is $B = 0.145818(6)$ cm^{-1}, which is now substantially smaller ($\Delta B/B = -0.40\%$) than the vibrationless ground state ($B_0 = 0.146414$ cm^{-1}). This contrasts dramatically with the uniformly positive $\Delta B/B$ values (see Table 3) for all the bending hot bands observed above,[29] and thus rules out assignment to the Σ−Σ component of the $4_0^1 7_2^2$ hot band. A strong *decrease* in B means that the effective moment of inertia along the molecular axis must *increase* significantly, which supports hot band assignment out of a collinear vibration with Σ symmetry. For example, excitation of the antisymmetric ν_4 CH stretch fundamental by itself yields $\Delta B/B = -0.15\%$, which one expects to grow further in magnitude for collinear stretching modes of the much heavier C atom framework.

Of the possible Σ symmetry vibrations, the one most comparable in energy to the four bending vibrations [see Table 1, 625(ν_6), 482(ν_7) and 627(ν_8), and 220(ν_9) cm^{-1}] would be the symmetric C−C stretching mode (ν_3) with a vibrational frequency of 871 cm^{-1}. Bizzocchi et al.[32] have extensively studied the ν_3 band of diacetylene at high resolution, and report that it is perturbed by $\sum_g^+$ symmetry sublevels of the combination $\nu_9 + \nu_8$ state and the $\nu_7 = 2$ level via three level resonance and anharmonic coupling. Their deperturbation analysis predicts $B = 0.146100$ cm^{-1} in the ν_3 excited state, which, as expected, is substantially lower than the vibrationless state but with $\Delta B = -3.11 \times 10^{-4}$ cm^{-1}, i.e., ≈ 2-fold smaller than the $\Delta B = -5.89 \times 10^{-4}$ cm^{-1} value observed experimentally. However, accurate ab initio vibration−rotation interaction coefficients have been calculated for diacetylene by Schaefer and co-workers,[55] which, as shown by Zhao et al.,[33] can be nicely exploited to identify the hot band assignment from shifts in precision rotational constants for the lower state. From the observed ΔB value, the potential vibrational candidates are therefore $4_0^1 2_1^1$ (symmetric triple CC bond stretch, $\Delta B \approx -6.5 \times 10^{-4}$ cm^{-1}) or $4_0^1 3_2^2$ (single CC bond stretch, $\Delta B \approx -6.3 \times 10^{-4}$ cm^{-1}), though absence of the corresponding single quantum $4_0^1 3_1^1$ hot band in our spectra would favor a $4_0^1 2_1^1$ assignment. Of dynamical interest is that the spectra provide unambiguous evidence for quite appreciable internal excitation of the newly formed diacetylene in both Σ (CC stretching) as well as Π (CCH, CCC bending) vibrational symmetries, even under slit jet expansion-cooled conditions.

E. Hot Vibrational versus Cold Rotational Populations. Observation of a series of ν_4-associated hot bands indicates the presence of non-negligible populations in each of the lower energy bending levels. Such a high degree of bending vibrational excitation is quite unexpected for a slit jet expansion, where the density drop off is much slower ($\propto 1/r$) than that of a pinhole expansion ($\propto 1/r^2$) and thus providing many orders of magnitude larger number of cooling collisions.[53,56] Indeed, slit cooling of vibrational populations for stable molecules with similar bending frequencies have routinely indicated nearly equilibrium behavior in slit jet expansions between rotational and vibrational degrees of freedom. Specifically, study of the bending vibration in jet-cooled CO_2, as well as an extensive progression of bending states in HF−CO_2 complexes, revealed essentially complete equilibrium between rotational, vibrational and even Doppler broadened translational temperatures as a function of distance downstream of the slit jet expansion orifice.[50−52] What makes the present situation different, of course, is that formation of diacetylene arises from reactive collisions (HCCH + CCH) in the discharge environment with potentially up to $\Delta H \approx -26$ kcal/mol energy release into products. Under these more enthalpically driven conditions, it is less obvious that the internal vibrational populations remain equilibrated with rotation/translation degrees of freedom and indeed can provide additional insight into the reaction dynamics.

To quantify this further, we consider a Boltzmann analysis for the vibrational ground state and each of the hot band lower vibrational levels, as determined by summation over the entire rovibrational band. For a system in thermal equilibrium, the integrated intensity for each rovibrational transition is described by[22]

$$S \propto p(v, J'')\cdot g_{nu}\cdot(2J''+1)\cdot A(J', J'')\cdot e^{-E_{rot}(v,J'')/kT}\cdot|\langle\psi'_{vib}|T|\psi''_{vib}\rangle|^2$$

where the relevant parameters are (i) lower rotational state population, (ii) nuclear spin weight, Hönl-London factor, Boltzmann factor, and vibrational transition moment, respectively. Note that the signals are summed over both *e* and *f* levels for unresolved or partially resolved lines in a Π−Π band. The resulting log−linear rotational Boltzmann plots for each of the vibrational bending manifolds are shown in Figure 4, which are consistent with a rotational temperature of $T_{rot} \approx 15 \pm 5$ K.

Similarly, relative vibrational populations can be readily obtained by summing up all rotational populations for a given vibrational manifold, where the ν_4 hot band transition dipole moment is assumed to be independent of the lower state. The resulting normalized populations for each vibrational level indicate that the ground state level clearly contains the dominant fraction (70%) of the total population, with the ν_6, ν_7, ν_8, and ν_9 bending modes populations estimated to be about 5.3%, 9.1%, 6.2%, and 1.7%, respectively. For the Σ−Σ band type progressions, the populations are estimated to be about 1.4% for $\nu_7 = 2$ and 3.6% for the tentatively assigned ν_2 or $2\nu_3$. These data can also be converted into a Boltzmann plot in Figure 5, which displays, with notable exception of lowest frequency (ν_9) bend excitation and the highest frequency CC stretch (ν_2 or $2\nu_3$) excitation, a behavior remarkably consistent with a vibrational "temperature" of $T_{vib} \approx 358(16)$ K. Though a somewhat different set of hot bands are observed and the vibrational temperatures reported are substantially higher ($T_{vib} \approx 580(50)$ K), these results are nevertheless in good qualitative agreement with conclusions of Zhao et al. for hot band

DOI: 10.1021/acs.jpca.5b02310
J. Phys. Chem. A 2015, 119, 7940−7950

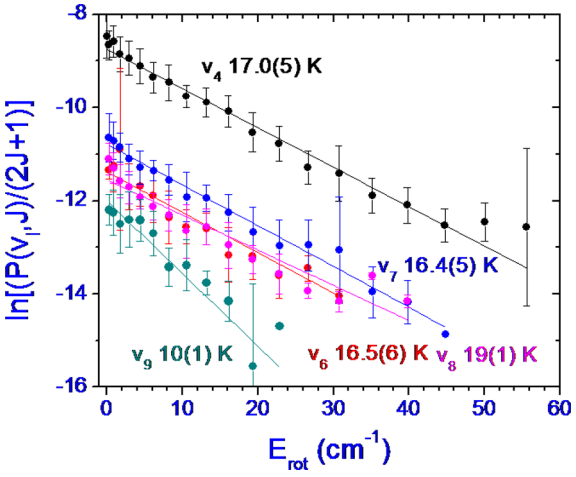

Figure 4. Boltzmann plot for the ν_4 fundamental mode as well as several of the many associated hot band bending levels. Note that the rotational temperature is quite consistent (T_{rot} = 15 ± 5 K) and well equilibrated between the multiple lower bending vibrational states (ν_6, ν_7, ν_8, and ν_9).

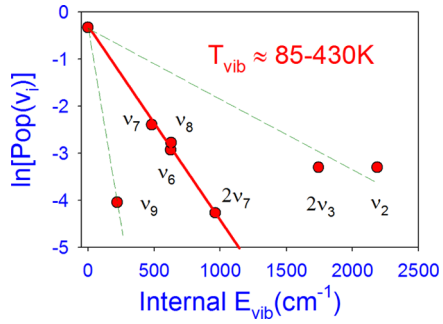

Figure 5. Boltzmann vibrational analysis for the various low lying Π bending states (ν_6, ν_7, ν_8, and ν_9), as well as the overtone $2\nu_7$ state and a previously unobserved collinear CC stretching vibration of Σ symmetry, which from band symmetry and ΔB for the lower state would indicate either $4_0^1 2_1^1$ or $4_0^1 3_2^2$. Note the remarkable linearity to the data for subset of states ν_6, ν_7, ν_8, also noted by Zhao et al.[33] Though the solid line through this subset of vibrational states correspond to ≈358(16) K, the dashed lines for both lower (ν_9) and higher (ν_2 or $2\nu_3$) frequencies would be consistent with a wider spread of "temperatures" from 85K to 430 K and thus incomplete equilibrium even in the vibrational manifold.

populations observed and assigned under different expansion conditions.[33] It is worth noting that the lowest (ν_9, 220 cm^{-1}) and highest (ν_2 or $2\nu_3$, 1700−2200 cm^{-1}) hot band frequencies deviate most significantly (T_{vib} ≈ 85 K vs 430 K) from this trend, which would indeed be consistent with differentially greater cooling efficiency in the slit jet expansion for lower versus higher vibrational frequencies. However, the key point of dynamical interest is that the degree of internal vibrational excitation for nascently formed diacetylene is substantially out of equilibrium with the much colder degrees of freedom associated with end-overend rotation, despite the much higher density of cooling collisions and efficient rovibrational equilibration routinely observed under slit jet expansion conditions.[50−52,56] This clearly points to a propensity for extensive internal vibrational excitation of the nascently formed diacetylene, i.e., in good agreement with the molecular beam studies of Kaiser et al. and ab initio theoretical support for which is discussed below.[6,7,19]

IV. DISCUSSION

The production chemistry and detection of diacetylene has been a subject of keen interest, due largely to its important role in terrestrial combustion, soot formation, and astrochemistry.[5,11,12,57−59] Successful spectroscopic detection of diacetylene in Titan's atmosphere was made possible by the strongly IR allowed ν_4 and ν_5 modes in the 3−5 μm region.[20,21,25,26] The work by Guelachvili et al. provided detailed information about these two fundamental bands, as well as a plethora of combination and difference bands built on low frequency bending vibrations populated under room temperature conditions.[29] Indeed, based on the vibrational frequencies in Table 1, the equilibrium population of the vibrational ground state should be ≈ 27% at 300 K, increasing rapidly to 92% for 100 K and essentially 100% for all temperatures below 50K, respectively. Under slit jet expansion conditions, therefore, one might expect the high density of cooling collisions to relax these low frequency bending excitations in particular, and thus collapse these extensive hot band spectra down to essentially the ν_4 fundamental. As evident in Figure 4, however, this is clearly not the case, and the high degree of disequilibrium between rotation (T_{rot} ≈15(5) K) and low frequency Σ, Π vibrations (T_{vib} ≈ 85−450 K) speaks to the extent of vibrational energy being pumped into these modes in the diacetylene formation event.

The reaction between the radical C_2H and the stable hydrocarbon C_2H_2 is one of the simplest neutral−neutral hydrocarbon reactions in chemical modeling of dense interstellar clouds. According to CCSD(T)/VtZ ab initio studies by Herbst and Woon[6] and confirmed by density functional theory (DFT) calculations by Kaiser et al.[7] the reaction of C_2H with C_2H_2 is initiated via enthalpically driven attack of radical to one of the carbon atoms in acetylene to form a stable C_s symmetry radical adduct 57 kcal/mol below the entrance asymptote. In particular, these theoretical studies predicted the absence of any incoming barrier in the entrance channel, which permitted calculation of temperature dependent rate constants by Herbst and Woon from long-range dipole-induced dipole capture theory.[6]

Of particular relevance to the present work, these CCSD(T) and DFT calculations not only predict the presence of a finite transition state in the exit channel, with a TS barrier height significantly below the HCC + HCCH reactant asymptote (−17.8 kcal/mol), but also significantly above (+7.5 kcal/mol) the exit channel to form HCCCCH + H products. Furthermore, the transition state geometry is planar (C_s) but with significantly bent (∠CCC ≈ 159°) and both longer and shorter (ΔCC ≈ +0.017 Å, −0.011 Å) CC bond lengths than in the product diacetylene (see Figure 6). For sufficiently "sudden" H atom escape from the transition state, this would be expected to result in Franck−Condon like vibrational excitation of the nascent diacetylene, with up to 7.5 kcal/mol excess energy stored in the TS geometry to be released into bending and stretching modes. Indeed, the radical intermediate is bent even further (∠CCC ≈ 122°) from collinear and with 5−10-fold larger deviations (ΔCC ≈ +0.112 Å, −0.059 Å) away from the asymptotic product CC bond lengths (see Figure 6), which would be dynamically consistent with a significant portion of the overall 25.6 kcal/mol exothermicity of the reaction funneling into bend and/or stretch vibration of the HCCCCH product. Either scenario would clearly predict anomalously high levels of vibrational bending and/or

DOI: 10.1021/acs.jpca.5b02310
J. Phys. Chem. A 2015, 119, 7940−7950

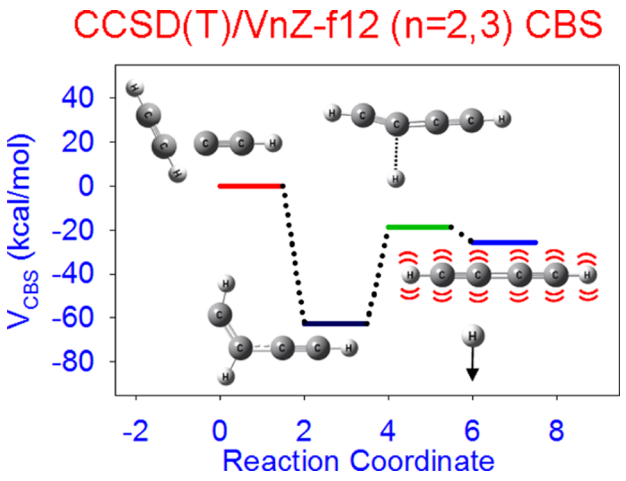

Figure 6. Potential energy critical points along the HCCH + CCH → HCCCCH + H reaction coordinate, calculated from high level MOLPRO CCSD(T) ab initio calculations using explicitly correlated V*n*Z-f12 (n = 2,3) basis sets, with the correlation energies extrapolated to the complete basis set limit (CBS).[40,41,60,61] Results with the improved basis set are fully consistent with previous work by Woon and Herbst,[6] and indicate the presence of strongly bent (i) stable HCCH−CCH radical intermediate (−62.6 kcal/mol) and (ii) a submerged transition state HCC(H)CCH (−18.9 kcal/mol) on the way to H atom ejection to form HCCCCH product (−25.6 kcal/mol). Note the strong noncolinearity in radical intermediate and transition state CCC bond angles, as well as deviations in CC single/triple bond lengths from diacetylene, which offer a simple dynamical picture for the extensive hot band structure observed experimentally.

stretching excitation in diacetylene, which is consistent with spectroscopic observations as well as molecular beam studies.[7,33] The presence of a submerged barrier in the ab initio calculations also implies that, at sufficiently low interstellar pressures and the absence of secondary collisions, the energized radical intermediate will fall apart with nearly unity quantum efficiency to form diacetylene.[6,7]

Under the much higher pressure conditions of a slit jet expansion or internal combustion environment, however, it becomes possible for collisions to remove this energy below the HCCCCH + H product asymptote and thereby stabilize the radical intermediate. Thus, it is of dynamical interest to estimate this complex dissociation lifetime,[13,14,19] and in particular whether slit jet collision frequencies are competitive with unimolecular rates for decomposition of the HCCH−CCH radical adduct. We have therefore calculated RRKM rate estimates for unimolecular dissociation over this submerged barrier (E_0) at some total energy $E_{tot} = E - E_0$. Specifically, we performed high level CCSD(T) ab initio calculations with the MOLPRO quantum chemistry software package,[40] using explicitly correlated f12 electron methods and specially optimized correlation consistent f12 basis sets of Peterson et al.[60] (V*n*Z-f12, n = 2,3) and a simple $1/n^3$ extrapolation of the correlation energies to the complete basis set (CBS) limit.[41,61] This permits us to extract zero point corrected energies and harmonic frequencies (see Figure 6 and Table 4) for each of (i) reactants (CCH + HCCH), (ii) the intermediate radical adduct (HCCH−CCH), (iii) the submerged transition state (TS) and (iv) diacetylene + H product species. These energy differences and vibrational frequencies in Table 4 are then used with the fundamental RRKM expression for unimolecular decomposition over a barrier, i.e., $k_{RRKM} = G^{\ddagger}(E - E_0)/h\rho(E)$, where E_0 = 37.8 kcal/mol is the zero point corrected barrier height, $\rho(E)$ the density of radical adduct states at internal energy E, and $G^{\ddagger}(E - E_0)$ represents the number of vibrational quantum states accessible at the TS barrier with an excess energy $E - E_0$.[42,43,62−67]

Table 4. Ab Initio Calculations (CCSD(T), MOLPRO Quantum Chemistry Package) for Reactant (HCCH + CCH), Intermediate Radical Adduct (HCCH−CCH), Transition State (HCC(H)CCH) and Product (HCCCCH + H) Species, Using Explicitly Correlated VTZ-f12 Basis Sets[a]

	CCSD(T)/vtz-f12				
frequencies (cm^{-1})	HCCH	CCH	adduct	TS	HCCCCH + H
	618.1	375.9	205.5	239.0	220.0
	618.1	375.9	322.7	242.9	220.0
	749.0	2022.7	498.0	482.5	481.1
	749.0	3444.9	626.7	488.9	481.1
	2006.9		656.5	551.8	642.1
	3410.0		690.6	617.7	642.1
	3501.9		866.3	641.8	643.0
			870.0	643.7	643.0
			994.3	646.3	891.4
			1265.5	899.3	2057.3
			1603.2	1981.9	2235.6
			2153.0	2201.2	3457.0
			3148.0	3435.4	3458.0
			3249.1	3457.6	
			3457.2	**1061.4i**	
ZPE (cm^{-1})	5826.5	3109.8	10303.2	8264.9	8035.8
ΔE+ΔZPE (kcal/mol)	0.0	0.0	−58.69	−20.89	−28.34

[a]Harmonic frequencies are reported in cm^{-1}, with the critical point energy differences corrected by harmonic zero point energies (ΔE + ΔZPE) and referenced with respect to the zero point level of the HCCH + CCH reactants. The imaginary frequency at the TS corresponds to the reaction coordinate. Note that the TS has a strongly submerged barrier with respect to incoming reactants and 7.45 kcal/mol above the product channel.

The resulting RRKM predictions for the unimolecular adduct decomposition rate constant as a function of internal energy E are displayed in Figure 7. If we treat the zero point corrected energy release associated with falling into the attractive well (−62.6 kcal/mol) as a lower limit on internal energy of the radical adduct (E = 58.4 kcal/mol), the corresponding fragmentation rate is predicted to be $k_{RRKM} \approx 2.8 \times 10^{10}$ 1/sec and $\approx 3.2 \times 10^{10}$ 1/s for VdZ-f12 and VtZ-f12 basis set levels, respectively. Even for typical gas kinetic rate constants of 2×10^{-10} cm^3/molecule/s and strong collision assumptions, stabilization of the radical adduct intermediate would still require considerably higher pressures of ≈ 4000 Torr or higher. As our slit jet typically operates at an order of magnitude *lower* pressures (300−500 Torr), this would be consistent with quite efficient (>90%) fragmentation of the adduct species to form the diacetylene product. However, these lifetime predictions also suggest that collisional quenching of the radical adduct could become an important channel at only moderately (10-fold) higher pressures, and therefore potentially important to a more detailed kinetic modeling of internal combustion dynamics.

As a parting comment, this CCH radical attack mechanism can continue further to form higher H-$(CC)_n$-H polyynes,

DOI: 10.1021/acs.jpca.5b02310
J. Phys. Chem. A 2015, 119, 7940−7950

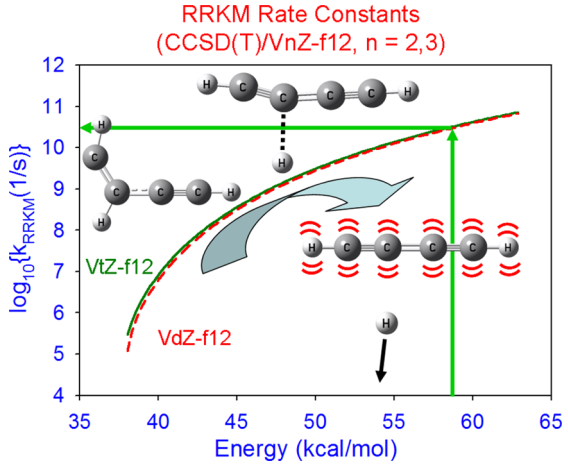

Figure 7. Internal energy dependent estimates of RRKM unimolecular decomposition rates for the HCCH−CCH radical complex formed by barrierless attack of CCH on HCCH, based on ab initio CCSD(T) calculations with explicitly correlated VnZ-f12 (n = 2,3) basis sets. The zero point corrected energy barrier from the complex to the transition state is E_0 = 37.8 kcal/mol, which for E = 58.7 kcal/mol internal energy corresponds to $k_{RRKM} = 3 \times 10^{10}$ 1/s and >10-fold faster than gas kinetic collision rates in the slit discharge expansion region.

provided there is sufficient time/collision frequency in the slit discharge expansion for additional CCH attack on diacetylene.[13,18] Indeed, we do see clear spectroscopic evidence in the infrared absorption spectrum for triacetylene formation in the relevant asymmetric CH stretch region, ostensibly via CCH addition to the initial diacetylene product. However, the above discussion raises an interesting point. The efficiency of such a radical extension mechanism to form successively longer polyynes depends on the ability of CCH (i) to insert in a barrierless fashion into a terminal H−C≡C−R bond and (ii) for the nascent radical adduct to dissociate over a barrier sufficiently submerged (i.e., small E_0) and with enough internal excitation (i.e., large E) to compete with vibrational relaxation processes via external collisions. This is clearly a highly efficient process at typical slit jet pressures for small H−C≡C−R reactant species (e.g., R = H, CCH). For sufficiently extended polyyne chain lengths, however, such a direct polyyne formation mechanism would be expected to become slower with respect to collisional relaxation.[13,14] Thus, one predicts under typical expansion and/or combustion conditions the possibility of rate limited termination to the polyyne chain extension kinetics, and thus the corresponding appearance of stabilized polyynic radical adducts amenable to further high resolution spectroscopic detection. However, theoretical and experimental work will be necessary to test the validity of these predictions.

V. SUMMARY AND CONCLUSIONS

In this report, the infrared spectroscopy of the C−H antisymmetric stretching mode (ν_4) of diacetylene and associated hot bands in the region of 3333 cm^{-1} is investigated with sub-Doppler resolution in a slit jet supersonic expansion and spectral analysis building on previous FTIR and cavity ring down studies.[29,33] The nascent species are formed in situ in the slit jet environment by discharge fragmentation of acetylene (HCCH) to form ethynyl radical (HCC) + H atoms, followed by barrierless attack of CCH with HCCH to form diacetylene prior to cooling in the subsequent expansion. Local rotational perturbative "crossings" in the ν_4 (Σ−Σ) fundamental band are observed for the first time and successfully analyzed based on simple Σ−Π Coriolis coupling. Evidence for extensive bending vibrational excitation of the diacetylene is also obtained, specifically by detection of ν_4 (Π−Π) hot bands built on each of the low frequency ν_6, ν_7, ν_8, and ν_9 bending vibrations, with spectroscopic analysis based on a weighted least-squares fit to a combined data set. Two additional hot bands of non-Π−Π vibrational symmetry are also observed and analyzed. One Δ−Δ band is readily identified by comparison with Zhao et al. as a ν_4 hot band built on two quanta of the ν_7 bend ($4_0^1 7_2^2$), for which the present work provides additional corroboration of the assignment.[33] In addition, a Σ−Σ ν_4 hot band is also observed, which, based on the decrease in the lower state rotational B constant ($\Delta B/B$ = −0.40%) and ab initio vibration−rotation interaction calculations,[55] suggests assignment to a hot band built on collinear CC stretching vibrations (e.g., ν_2 or $2\nu_3$) of Σ symmetry. Lower state rovibrational populations from these hot bands are analyzed via Boltzmann analysis, which provides evidence for quite hot distributions of Π and Σ vibrations in formation of the nascent diacetylene considerably out of equilibrium with the observed rotational temperatures (15 ± 5 K) despite the much higher number of cooling collisions in the slit jet expansion environment. The results are in good agreement with the translational energy distributions noted in molecular beam studies by Kaiser et al, which indicate more than 50% ($E_{int} \approx 14 \pm 3$ kcal/mol) of the available exothermicity (E_{max} = 26.7 kcal/mol) remaining in the nascently formed diacetylene.[7]

Potential dynamical reasons for such highly vibrationally diacetylene distributions are explored using high level CCSD(T) calculations with explicitly correlated VnZ-f12 (n = 2,3) basis sets, for which correlation energies have been extrapolated to the complete basis set limit (CBS). The results indicate strongly bent radical adduct and transition state geometries, supporting the work of Herbst and Woon[6] and Kaiser et al.[7] and offer a simple physical model for funneling of the reaction exothermicity into CH/CCC bending and CC stretching modes of the nascent diacetylene product. Finally, CCSD(T)/VtZ-f12 vibrational zero point corrected energies and frequencies at the intermediate and transition state geometries have been exploited for predicting RRKM dissociation lifetimes of the HCCH−CCH radical complex. These lifetimes are consistent with a high quantum yield (> 90%) of diacetylene formation in a typical low pressure slit jet expansion, but also predict collisional stabilization of the radical complex to be a potentially important channel under the higher pressure conditions relevant to internal combustion processes.

AUTHOR INFORMATION

Corresponding Author

*E-mail: djn@jila.colorado.edu; Tel: 303-492-8857.

Notes

The authors declare no competing financial interest.

ACKNOWLEDGMENTS

This work was supported by grants from the Department of Energy (DE-FG02-09ER16021), with funds for construction of the slit jet laser spectrometer provided by the National Science Foundation (CHE 1266416, PHY 1125844). We would also like to acknowledge Melanie Roberts and Grant Buckingham

DOI: 10.1021/acs.jpca.5b02310
J. Phys. Chem. A 2015, 119, 7940−7950

for assistance with the slit jet spectrometer and acquisition of the spectral data.

REFERENCES

(1) Ceursters, P.; Nguyen, H. M. T.; Peeters, J.; Nguyen, M. T. Experimental and Theoretical Study of the Reaction of the Ethynyl Radical with Acetylene. *Chem. Phys.* **2000**, *262*, 243−252.

(2) Wagner, A. F. The Challenges of Combustion for Chemical Theory. *Proc. Combustion Inst.* **2002**, *29*, 1173−1200.

(3) Harding, L. B.; Wagner, A. F. Theoretical Studies on the Reaction of Atomic Oxygen ($O(^3P)$) with Acetylene. II. *J. Phys. Chem.* **1986**, *90*, 2974−2987.

(4) Michael, J. V.; Su, M. C.; Sutherland, J. W.; Harding, L. B.; Wagner, A. F. Rate Constants for $D+C_2H_2 \rightarrow C_2HD+H$ at High Temperature: Implications to the High Pressure Rate Constant for $H+C_2H_2 \rightarrow C_2H_3$. *J. Phys. Chem. A* **2003**, *107*, 10533−10543.

(5) Baulch, D. L.; Cobos, C. J.; Cox, R. A.; Esser, C.; Frank, P.; Just, T.; Kerr, J. A.; Pilling, M. J.; Troe, J.; Walker, R. W. Evaluated Kinetic Data for Combustion Modeling. *J. Phys. Chem. Ref. Data* **1992**, *21*, 411−734.

(6) Herbst, E.; Woon, D. E. The Rate of the Reaction between C_2H and C_2H_2 at Interstellar Temperatures. *Astrophys. J.* **1997**, *489*, 109−112.

(7) Kaiser, R. I.; Stahl, F.; Schleyer, P. V.; Schaefer, H. F. Atomic and Molecular Hydrogen Elimination in the Crossed Beam Reaction of d_1-Ethynyl Radicals $C_2D(X\ ^2\Sigma^+)$ with Acetylene, $C_2H_2(X\ ^1\Sigma^+_g)$: Dynamics of d_1-Diacetylene (HCCCCD) and d_1-Butadiynyl (DCCCC) Formation. *Phys. Chem. Chem. Phys.* **2002**, *4*, 2950−2958.

(8) Vakhtin, A. B.; Heard, D. E.; Smith, I. W. M.; Leone, S. R. Kinetics of Reactions of C_2H Radical with Acetylene, O_2, Methylacetylene, and Allene in a Pulsed Laval Nozzle Apparatus at T = 103 K. *Chem. Phys. Lett.* **2001**, *344*, 317−324.

(9) Vanlook, H.; Peeters, J. Rate Coefficient of the Reactions of C_2H with O_2, C_2H_2 and H_2O between 295 and 450K. *J. Phys. Chem.* **1995**, *99*, 16284−16289.

(10) Pino, T.; Ding, H. B.; Guthe, F.; Maier, J. P. Electronic Spectra of the Chains $HC_{2n}H$ (n = 8−13) in the Gas Phase. *J. Chem. Phys.* **2001**, *114*, 2208−2212.

(11) Frenklach, M. Reaction Mechanism of Soot Formation in Flames. *Phys. Chem. Chem. Phys.* **2002**, *4*, 2028.

(12) McEnally, C. S.; Pfefferle, L. D.; Atakan, B.; Kohse-Hoeinghaus, K. Studies of Aromatic Hydrocarbon Formation Mechanisms in Flames: Progress Towards Closing the Fuel Gap. *Prog. Energy Combust. Sci.* **2006**, *32*, 247.

(13) Jamal, A.; Mebel, A. M. An Ab Initio/RRKM Study of the Reaction Mechanism and Product Branching Ratios of the Reactions of Ethynyl Radical with Allene and Methylacetylene. *Phys. Chem. Chem. Phys.* **2010**, *12*, 2606−2618.

(14) Jamal, A.; Mebel, A. M. Reactions of C_2H with 1-and 2-Butynes: An Ab Initio/RRKM Study of the Reaction Mechanism and Product Branching Ratios. *J. Phys. Chem. A* **2011**, *115*, 2196−2207.

(15) Vuitton, V.; Scemama, A.; Gazeau, M. C.; Chaquin, P.; Bénilan, Y. IR and UV Spectroscopic Data for Polyynes: Predictions for Long Carbon Chain Compounds in Titan's Atmosphere. *Adv. Space Res.* **2001**, *27*, 283.

(16) Allen, M.; Pinto, J. P.; Yung, Y. L. Titan - Aerosol Photochemistry and Variations Related to the Sunspot Cycle. *Astrophys. J.* **1980**, *242*, L128.

(17) Khlifi, M.; Paillous, P.; Delpech, C.; Nishio, M.; Bruston, P.; Raulin, F. Absolute IR Band Intensities of Diacetylene in the 250−4300 cm^{-1} Region: Implications for Titan's Atmosphere. *J. Mol. Spectrosc.* **1995**, *174*, 116.

(18) Gu, X.; Kim, Y. S.; Kaiser, R. I.; Mebel, A. M.; Liang, M. C.; Yung, Y. L. Chemical Dynamics of Triacetylene Formation and Implications to the Synthesis of Polyynes in Titan's Atmosphere. *Proc. Natl. Acad. Sci. U. S. A.* **2009**, *106*, 16078−16083.

(19) Le, T. N.; Mebel, A. M.; Kaiser, R. I. Ab Initio Study of C_4H_3 Potential Energy Surface and Reaction of Ground-State Carbon Atom with Propargyl Radical. *J. Comput. Chem.* **2001**, *22*, 1522−1535.

(20) Lavvas, P. P.; Coustenis, A.; Vardavas, I. M. Coupling Photochemistry with Haze Formation in Titan's Atmosphere, Part I: Model Description. *Planet. Space Sci.* **2008**, *56*, 27.

(21) Wilson, E. H.; Atreya, S. K. Chemical Sources of Haze Formation in Titan's Atmosphere. *Planet. Space Sci.* **2003**, *51*, 1017.

(22) Bunker, P. R.; Jensen, P. *Molecular Symmetry and Spectroscopy*, 2nd ed.; NRC Research Press: Ottawa, Canada, 1998.

(23) Townes, C. H.; Schawlow, A. L. *Microwave Spectroscopy*, 1st ed.; McGraw-Hill Book Company: New York, 1955.

(24) Kunde, V. G.; Aikin, A. C.; Hanel, R. A.; Jennings, D. E.; Maguire, W. C.; Samuelson, R. E. C_4H_2, HC_3N and C_2N_2 in Titan's Atmosphere. *Nature* **1981**, *292*, 686.

(25) Porco, C. C.; Baker, E.; Barbara, J.; Beurle, K.; Brahic, A.; Burns, J. A.; Charnoz, S.; Cooper, N.; Dawson, D. D.; Del Genio, A. D. Imaging of Titan from the Cassini Spacecraft. *Nature* **2005**, *434*, 159.

(26) Coustenis, A.; Bezard, B.; Gautier, D.; Marten, A.; Samuelson, R. Titan's Atmosphere from Voyager Infrared Observations. III. Vertical Distributions of Hydrocarbons and Nitriles near Titan's Northpole. *Icarus* **1991**, *89*, 152−167.

(27) Waite, J. H.; Young, D. T.; Cravens, T. E.; Coates, A. J.; Crary, F. J.; Magee, B.; Westlake, J. The Process of Tholin Formation in Titan's Upper Atmosphere. *Science* **2007**, *316*, 870−875.

(28) Shindo, F.; Bénilan, Y.; Chaquin, P.; Guillemin, J. C.; Jolly, A.; Raulin, F. IR Spectrum of C_8H_2: Integrated Band Intensities and Some Observational Implications. *J. Mol. Spectrosc.* **2001**, *210*, 191.

(29) Guelachvili, G.; Craig, A. M.; Ramsay, D. A. High-Resolution Fourier Studies of Diacetylene in the Regions of the ν_4 and ν_5 Fundamentals. *J. Mol. Spectrosc.* **1984**, *105*, 156.

(30) Arie, E.; Johns, J. W. C. The Bending Energy Levels of C_4H_2. *J. Mol. Spectrosc.* **1992**, *155*, 195.

(31) Bizzocchi, L.; Esposti, C. D.; Dore, L. Submillimetre-Wave Spectrum of Diacetylene and Diacetylene-d_2. *Mol. Phys.* **2010**, *108*, 2315.

(32) Bizzocchi, L.; Tamassia, F.; Esposti, C. D.; Fusina, L.; Cane, E.; Dore, L. High-Resolution Infrared Spectroscopy of Diacetylene Below 1000 cm^{-1}. *Mol. Phys.* **2011**, *109*, 2181.

(33) Zhao, D.; Doney, K. D.; Linnartz, H. High-Resolution Infrared Spectra of Vibrationally Excited HC_4H in a Supersonic Hydrocarbon Plasma. *J. Mol. Spectrosc.* **2014**, *296*, 1−8.

(34) Matsumura, K.; Kanamori, H.; Kawaguchi, K.; Hirota, E.; Tanaka, T. Infrared Diode Laser Spectroscopy of Triacetylene by the Source and the Stark Modulation Techniques. *J. Mol. Spectrosc.* **1988**, *131*, 278.

(35) McNaughton, D.; Bruget, D. N. The High-Resolution Infrared Spectrum of Triacetylene. *J. Mol. Spectrosc.* **1991**, *150*, 620.

(36) Matsumura, K.; Etoh, T.; Tanaka, T. Microwave Spectroscopy of the ν_8−ν_6 Band of Diacetylene. *J. Mol. Spectrosc.* **1981**, *90*, 106.

(37) Matsumura, K.; Kawaguchi, K.; Hirota, E.; Tanaka, T. Stark Modulation Infrared Diode Laser Spectroscopy of the $\nu_6 + \nu_8$ Band of Diacetylene. *J. Mol. Spectrosc.* **1986**, *118*, 530.

(38) Matsumura, K.; Tanaka, T. The Effect of Bending Vibrations on the Dipole Moment of a Linear Polyatomic Molecule: A Theoretical Treatment of the Vibrational Changes and Transition Moments. *J. Mol. Spectrosc.* **1986**, *116*, 320.

(39) Matsumura, K.; Tanaka, T. The Effect of Bending Vibrations on the Dipole Moment of a Linear Polyatomic Molecule: Analysis of the Vibrational Changes and Transition Moments for Acetylene and Diacetylene. *J. Mol. Spectrosc.* **1986**, *116*, 334.

(40) Werner, H.-J.; Knowles, P. J.; Lindh, R.; Manby, F. R.; M. Schütz; Celani, P.; Korona, T.; Mitrushenkov, A.; Rauhut, G.; T. B. Adler Molpro, Version 2009.1, A Package of *Ab Initio* Programs; see http://www.molpro.net, 2009.

(41) Peterson, K. A.; Woon, D. E.; Dunning, T. H. Benchmark Calculations with Correlated Molecular Wave-Functions.IV. The Classical Barrier Height of the $H+H_2 \rightarrow H_2+H$ Reaction. *J. Chem. Phys.* **1994**, *100*, 7410−7415.

(42) Levine, R. D.; Bernstein, R. B. *Molecular Reaction Dynamics and Chemical Reactivity*; Oxford, 1987.

DOI: 10.1021/acs.jpca.5b02310
J. Phys. Chem. A 2015, 119, 7940−7950

(43) Robinson, P. J.; Holbrook, K. A. *Unimolecular Reactions*; Wiley-Interscience: London, 1972.
(44) Anderson, D. T.; Davis, S.; Zwier, T. S.; Nesbitt, D. J. An Intense Slit Discharge Source of Jet-Cooled Molecular Ions and Radicals (T_{rot} < 30 K). *Chem. Phys. Lett.* **1996**, *258*, 207.
(45) Davis, S.; FárnIk, M.; Uy, D.; Nesbitt, D. J. Concentration Modulation Spectroscopy with a Pulsed Slit Supersonic Discharge Expansion Source. *Chem. Phys. Lett.* **2001**, *344*, 23.
(46) Sharp-Williams, E. N.; Roberts, M. A.; Nesbitt, D. J. High Resolution Slit-Jet Infrared Spectroscopy of Ethynyl Radical: $^2\Pi \leftarrow {}^2\Sigma^+$ Vibronic Bands with Sub-Doppler Resolution. *J. Chem. Phys.* **2010**, *134*, 064314.
(47) Vanderauwera, J.; Hurtmans, D.; Carleer, M.; Herman, M. The N_3 Fundamental in C_2H_2. *J. Mol. Spectrosc.* **1993**, *157*, 337.
(48) Brown, J. M.; Hougen, J. T.; Huber, K. P.; Johns, J. W. C.; Kopp, I.; Lefebvre-Brion, H.; Merer, A. J.; Ramsay, D. A.; Rostas, J.; Zare, R. N. The Labeling of Parity Doublet Levels in Linear Molecules. *J. Mol. Spectrosc.* **1975**, *55*, 500.
(49) Herzberg, G. *Infrared and Raman Spectra of Polyatomic Molecules*; D. Van Nostrand Company, Inc.: New York, 1945; Vol. *II*.
(50) Lovejoy, C. M.; Nesbitt, D. J. High Sensitivity, High-Resolution IR Laser Spectroscopy in Slit Supersonic Jets: Application to N_2HF ν_1 and $\nu_5+\nu_1-\nu_5$. *J. Chem. Phys.* **1987**, *86*, 3151−3165.
(51) Lovejoy, C. M.; Schuder, M. D.; Nesbitt, D. J. Direct Ir Laser-Absorption Spectroscopy of Jet-Cooled CO_2HF Complexes: Analysis of the ν_1 HF Stretch and a Surprisingly Low-Frequency ν_6 Intermolecular CO_2 Bend. *J. Chem. Phys.* **1987**, *86*, 5337−5349.
(52) Nesbitt, D. J.; Lovejoy, C. M. Multiple Intermolecular Bend Vibrational-Excitation of a Hydrogen-Bond: An Extended Infrared Study of OCOHF. *J. Chem. Phys.* **1990**, *93*, 7716−7730.
(53) Courreges-Lacoste, G. B.; Sprengers, J. P.; Ubachs, W.; Stolte, S.; Linnartz, H. The $A^2\Sigma^+ \leftarrow X\ ^2\Pi$ Transition of CF Starting from Highly Excited Vibrational States. *J. Mol. Spectrosc.* **2001**, *205*, 341−343.
(54) Wang, S. C. On the Asymmetrical Top in Quantum Mechanics. *Phys. Rev.* **1929**, *34*, 243−252.
(55) Simmonett, A. C.; Schaefer, H. F.; Allen, W. D. Enthalpy of Formation and Anharmonic Force Field of Diacetylene. *J. Chem. Phys.* **2009**, *130*, 044301.
(56) Lovejoy, C. M.; Nesbitt, D. J. Slit Pulsed Valve for Generation of Long-Path-Length Supersonic Expansions. *Rev. Sci. Instrum.* **1987**, *58*, 807−811.
(57) Senosiain, J. P.; Klippenstein, S. J.; Miller, J. A. Oxidation Pathways in the Reaction of Diacetylene with OH Radicals. *Proc. Combustion Inst.* **2007**, *31*, 185.
(58) McEnally, C. S.; Pfefferle, L. D.; Robinson, A. G.; Zwier, T. S. Aromatic Hydrocarbon Formation in Nonpremixed Flames Doped with Diacetylene, Vinylacetylene, and Other Hydrocarbons: Evidence for Pathways Involving C_4 Species. *Combust. Flame* **2000**, *123*, 344.
(59) Kaiser, R. I.; Sun, B. J.; Lin, H. M.; Chang, A. H. H.; Mebel, A. M.; Kostko, O.; Ahmed, M. An Experimental and Theoretical Study on the Ionization Energies of Polyynes $(H-(CC)_n-H;\ n = 1-9$. *Astrophys. J.* **2010**, *719*, 1884.
(60) Peterson, K. A.; Adler, T. B.; Werner, H.-J. Systematically Convergent Basis Sets for Explicitly Correlated Wavefunctions: The Atoms H, He, B−Ne, and Al−Ar. *J. Chem. Phys.* **2008**, *128*, 084102.
(61) Peterson, K. A.; Kendall, R. A.; Dunning, T. H. Benchmark Calculations with Correlated Molecular Wave-Functions. II. Configuration-Interaction Calculations on 1st Row Diatomic Hydrides. *J. Chem. Phys.* **1993**, *99*, 1930−1944.
(62) Houston, P. L. *Chemical Kinetics and Reaction Dynamics*; McGraw-Hill: New York, 2001.
(63) Kassel, L. S. Studies in Homogeneous Gas Reactions I. *J. Phys. Chem.* **1928**, *32*, 225−242.
(64) Kassel, L. S. Studies in Homogeneous Gas Reactions II Introduction of Quantum Theory. *J. Phys. Chem.* **1928**, *32*, 1065−1079.
(65) Marcus, R. A. Unimolecular Dissociations and Free Radical Recombination Reactions. *J. Chem. Phys.* **1952**, *20*, 359−364.
(66) Rice, O. K.; Ramsperger, H. C. Theories of Unimolecular Gas Reactions at Low Pressures. *J. Am. Chem. Soc.* **1927**, *49*, 1617−1629.
(67) Rice, O. K.; Ramsperger, H. C. Theories of Unimolecular Gas Reactions at Low Pressures II. *J. Am. Chem. Soc.* **1928**, *50*, 617−620.

DOI: 10.1021/acs.jpca.5b02310
J. Phys. Chem. A 2015, 119, 7940−7950